Chord rotation demand for Effective Catenary Action under Monotonic

Loadings

†*Meng-Hao Tsai

Department of Civil Engineering, National Pingtung University of Science and Technology, Taiwan.

 $\label{lem:pustedutw} $$ *Presenting author: mhtsai@mail.npust.edu.tw $$ $ $ *Corresponding author: mhtsai@mail.npust.edu.tw $$$

Abstract

In the past decade, several experimental and numerical studies were conducted with reinforced concrete (RC) beam-column sub-assemblages to investigate the progressive collapse resistance of frame structures under column loss. Most of the studies suggested that the catenary action could be used as the final defensive mechanism against collapse. However, it was observed from the loaddeflection curves that there was a strength-decreased transition phase between the peak arch resistance and the commencement of catenary action. This transition region may imply an unstable snap-through behavior under a real dynamic column loss scenario. Hence, the chord rotation demands for effective catenary action of RC beams were investigated in this study. The nonlinear static load-deflection response of RC beam-column sub-assemblages under gravitationally monotonic loadings was idealized as a piecewise linear curve divided by the yield strength, peak arch resistance, leveled-off strength, and peak catenary resistance before bar fracture. The corresponding pseudo-static load response was then analytically derived for each linear region. Based on the analytical formulation, numerical analyses were carried out to understand the variation of the chord rotation demand with some key parameters related to the collapse-resistant performance. Parametric study results indicated that smaller peak-arch rotation and larger catenary stiffness could induce less rotation demand for the effective catenary action. This implies that RC beams with a deep section require larger rotation capacity for the effective catenary action. Since RC members with a deep section are usually responsible of large shear and/or moment, it is suggested that their peak arch strength is used as the collapse resistance for the sake of safety. Also, a peak-arch strength recovery in the nonlinear static response curve does not always guarantee a similar strength recovery in the pseudo-static counterpart. Complementary pseudo-static analysis is advised to verify the effective catenary action under realistic dynamic column loss.

Keywords: Progressive collapse, Effective catenary action, Pseudo-static response, Chord rotation

Introduction

Progressive collapse vulnerability of building structures has become an active research topic since the 9/11 terrorism attack of the World Trade Center in 2001. As stated in the ASCE 7-10 Standard [ASCE (2010)], progressive collapse is defined as "the spread of an initial local failure from element to element, resulting eventually in the collapse of an entire structure or a disproportionately large part of it". Therefore, it is sometime indicated as "disproportional collapse". Several experimental studies were performed with beam-column sub-assemblages, as shown in Fig.1, to investigate the progressive collapse resistance of frame structures in the past decade. Su et al. (2009) performed static vertical loading tests on twelve longitudinally restrained RC beams with varied steel ratios and span-to-depth ratios. The tested specimens generally reached peak compressive arch strength at a deflection ranging from 16% to 34% of section depth. For some specimens, the load resistance in catenary stage may be lower than the arch strength. Sasani et al. (2011) adopted a 3/8 scaled sub-assemblage to evaluate the column-loss response of an RC beam bridging over the removed column. Choi and Kim (2011) performed static loading tests on reduced-scale RC sub-assemblages designed with and without seismic detailing and concluded that significant catenary action may be activated for seismically detailed beams. Some dynamic loading tests have been

carried out to investigate the dynamic column-loss response of RC beam-column sub-assemblages and structural frames [Tian and Yu (2011), Qian and Li (2012), Orton and Kirby (2014)]. Yu and Tan (2013) designed eight RC sub-assemblage specimens with varied steel ratios and span-to-depth ratios to study the ultimate catenary resistance under column loss.

Most of the experiments suggested that the catenary action could be used as the final defensive mechanism against collapse. They also revealed that development of the catenary action was dependent on the beam-end rotational capacity. Hence, the design guidelines issued by the US General Service Administration [GSA (2003)] and the Department of Defense [DoD (2005), (2009)] have proposed an acceptance criterion of 0.20 radians for the chord rotation of the two-span beams, as defined in Fig. 1, in nonlinear progressive collapse analysis of RC frames. This threshold was specified independent of structural parameters. However, from those referred experimental studies, the rotational demands corresponding to the peak arch strength, commencement of catenary action, and bar-fracture strength were varied. Hence, analytical resolution of the rotational demands for effective catenary action of progressive collapse is proposed in this study. Piecewise linear curves divided by the yield strength, peak arch resistance, leveled off strength, and peak catenary resistance were used at first to idealize the general nonlinear static response of RC beam-column sub-assemblages under gravitationally monotonic loadings. Then, the corresponding pseudo-static load response was analytically derived for each linear region. A definition for the effective catenary action was described. The analytical expressions were used to carry out numerical investigations on the chord rotation demands of the effective catenary action and associated snap-through response. Practical implications were drawn based on the numerical analysis results.

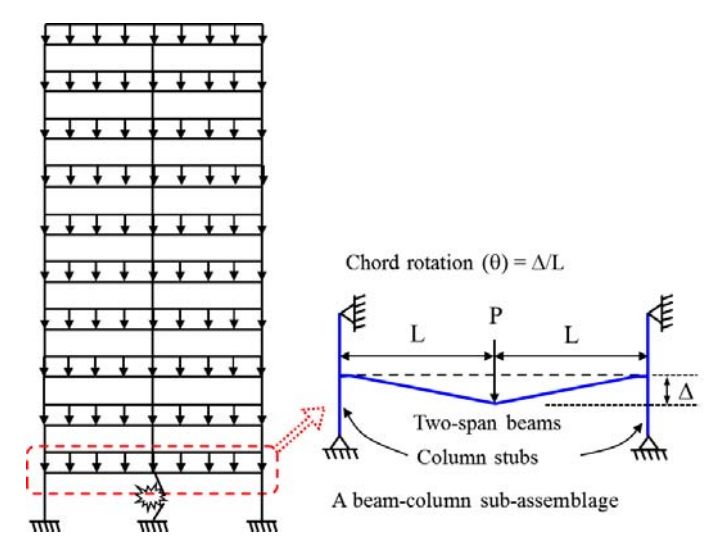


Figure 1 The definition of a beam-column sub-assemblage

Idealization of Static Response

From the results of most monotonic static loading tests, it was revealed that the load-deflection responses of RC beam-column sub-assemblage specimens were highly nonlinear. The nonlinear static response was initiated at the tensile cracking of concrete and grew significantly as the tensile reinforcement yielded. Along with the flexural yielding, the load response gradually increased to the so-called peak arch resistance, as shown in Fig. 2(a). This load-deflection range may be defined as the "compressive arch" phase. In this phase, compressive axial force is developed in the beam members of the RC sub-assemblage due to the restraint provided by the end columns. From most of the experimental and numerical studies, it was observed that there is a strength-decreased transition phase after the peak arch resistance. It is defined as the "transition phase". This strength-decreased

region may induce snap-through response under a real dynamic column loss scenario [Tsai (2012), Orton and Kirby (2014)]. Analytical and numerical studies [Tsai and Lin (2008), Tsai (2010), Tsai and You (2012)] have indicated that pseudo-static response obtained from the nonlinear static load-deflection curve may be used to predict the maximum dynamic response under column loss. As the supported loading is larger than the dynamic peak arch resistance, the beam-column sub-assemblage will be loaded directly into the catenary phase and significantly large deformation could be induced under column loss. This reveals that the peak arch resistance is an important threshold for the snap-through behavior. In this phase, the load resistance may gradually decrease and level off at P_c , where the catenary action is activated. The load resistance may be regained under the catenary action until any of the steel bars fails in rupture and this region is thus defined as the "catenary phase". Axial tension is developed in the beam members during the catenary phase and provides the collapse resistance for the two-span beams.

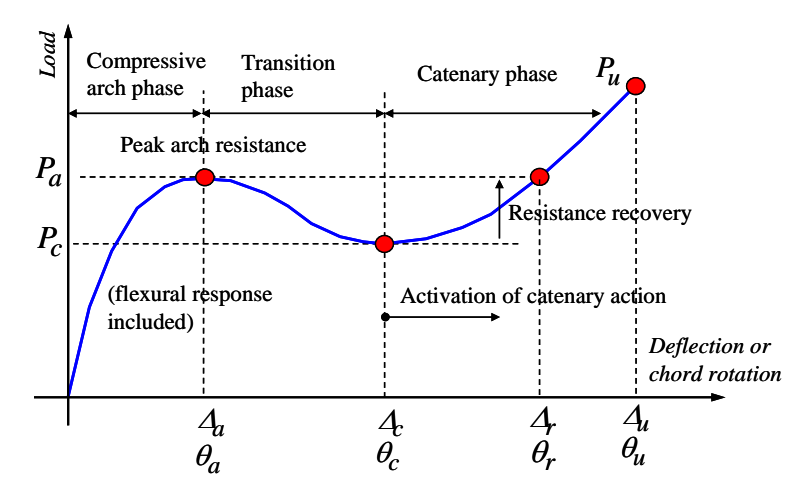


Figure 2(a) Static load-deflection curve under gravitational monotonic loadings

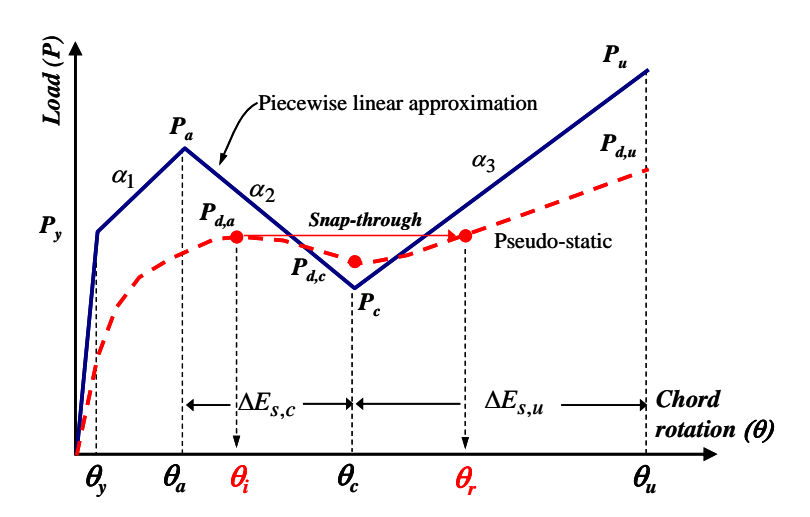


Figure 2(b) Idealized piece-wise linear curve and pseudo-static response

Although the general static load-deflection curve is nonlinear, as a rule of thumb, it can be approximated as piece-wise linear response with four threshold points, as shown in Fig. 2(b). The four threshold points are corresponding to the yielding strength, peak arch resistance, leveled off strength, and peak catenary resistance before bar fracture. As shown in the figure, the stiffness

ratios of the three post-yield regions to the elastic stiffness are designated by α_1 , α_2 , and α_3 . α_1 is defined as the arch stiffness ratio ranging from the yield point to the peak arch resistance. α_2 is defined as the softening stiffness ratio ranging from the peak arch resistance to the leveled off point. α_3 is defined as the catenary stiffness ratio for the catenary phase. With these parameters, the analytical pseudo-static response in each phase can be obtained for the idealized nonlinear static curve.

Analytical pseudo-static response

The pseudo-static loading may be numerically obtained from dividing the accumulated area under the nonlinear static load-displacement curve by the corresponding displacement of the column-loss point. Mathematically, it may be expressed as

$$P_{CC}(u_d) = \frac{1}{u_d} \int_{0}^{u_d} P_{NS}(u) du$$
 (1)

where $P_{CC}(u)$ and $P_{NS}(u)$ are, respectively, the pseudo-static loading and the nonlinear static loading at the displacement demand u. For the idealized nonlinear static response, the pseudo-static force in the elastic range may be written as

$$P_{d,0} = P/2, \ 0 \le P \le P_{y}$$
 (2)

where P_y is the static yielding force. From the yield point to the peak arch resistance, it is derived that the pseudo-static force $P_{d,2}$ can be expressed as

$$P_{d,1} = \frac{P_y[\alpha_1(\mu - 1)^2 + 2(\mu - 1) + 1]}{2\mu}, \ 1 \le \mu \le \mu_a$$
 (3)

where the ductility, μ , is the chord rotation divided by the yield rotation θ_y . $\mu_a = \theta_a/\theta_y$, which denotes the ductility demand at the peak arch resistance P_a (Fig. 2(b)). Similarly, the pseudo-static forces in the transition and catenary phases are respectively derived as

$$P_{d,2} = \frac{P_{d,a}\mu_a}{\mu} + \frac{P_y[-\alpha_2(\mu - \mu_a)^2 + 2(\mu - \mu_a)[1 + \alpha_1(\mu_a - 1)]]}{2\mu}, \ \mu_a \le \mu \le \mu_c$$
 (4)

and

$$P_{d,3} = \frac{P_{d,c}\mu_c}{\mu} + \frac{P_y[\alpha_3(\mu - \mu_c)^2 + 2(\mu - \mu_c)[1 + \alpha_1(\mu_a - 1) - \alpha_2(\mu_c - \mu_a)]]}{2\mu}, \ \mu_c \le \mu$$
 (5)

where $P_{d,a} = P_{d,1}(\mu = \mu_a)$ and $P_{d,c} = P_{d,2}(\mu = \mu_c)$. $\mu_c = \theta_c/\theta_y$, which represents the ductility demand at the end of transition phase. A general form for the pseudo-static force in the i-th linear region and $i \ge 2$ may be deduced from the above equations as

$$P_{d,i} = \frac{P_{d,i-1}(\mu_{i-1}) \cdot \mu_{i-1}}{\mu} + \frac{P_y[\alpha_i(\mu - \mu_{i-1})^2 + 2(\mu - \mu_{i-1})[1 + \sum_{j=1}^{i-1} \alpha_j(\mu_j - \mu_{j-1})]]}{2\mu}, \ \mu_{i-1} \le \mu$$
 (6)

where μ_{i-1} is the ductility demand of the previous turning point and the sign of stiffness is included in the ratios α_i and α_i .

As shown in Fig. 2(b), the pseudo-static peak arch resistance, denoted as $P_{p,a}$, does not occur at the chord rotation θ_a corresponding to its static counterpart. Instead, it happens during the transition phase, ie. in the range from θ_a to θ_c . From setting the derivative of Eq.(4) equal to zero, it can be obtained that $P_{p,a}$ occurs at

$$\mu = \mu_i = \sqrt{\frac{(\alpha_2 + 2\alpha_1)\mu_a^2 + 2(1 - \alpha_1)\mu_a}{\alpha_2}}$$
 (7)

The value of $P_{p,a}$ is then calculated as $P_{d,2}(\mu=\mu_i)$. The chord rotation at μ_i is denoted as θ_i in Fig. 2(b). This rotation is defined as the snap-through prevention limit. It can be regarded as an index to judge the importance of the catenary action. If θ_i is larger than the expected beam-end rotation, the catenary action will be minor under the column loss. Moreover, from the comparison of the nonlinear static and pseudo-static load-deflection curves, it is clear that if the static leveled off rotation θ_c is less than θ_i , then the pseudo-static response shall be a non-degrading curve with non-negative tangent stiffness. In such a case, there will be no snap-through response under dynamic column loss [Tsai (2012)] and the catenary action is always effective in enhancing the collapse resistance. However, as θ_c is larger than θ_i , the pseudo-static resistance mayl be lower than $P_{p,a}$ and the snap-through response will be induced consequently. Once it happens, the dynamically falling behavior can be arrested only if the resistance of $P_{p,a}$ may be regained in the catenary phase. Otherwise, dynamic collapse will happen. Therefore, an effective catenary action is defined as the capability of recovering the strength of $P_{p,a}$ in the catenary phase. The chord rotation demand for the effective catenary action is then determined from $P_{d,3} \ge P_{p,a}$, which leads to

$$A\mu^2 + B\mu + C \ge 0 \tag{8}$$

where $A = \alpha_3$, $B = 2[1 + \alpha_1(\mu_a - 1) - \alpha_2(\mu_c - \mu_a) - \alpha_3\mu_c - 2P_{d,i}/P_y]$, and

$$C = \alpha_3 \mu_c^2 - 2\mu_c [1 + \alpha_1(\mu_a - 1) - \alpha_2(\mu_c - \mu_a) - 2P_{d,c} / P_y] \ge 0.$$

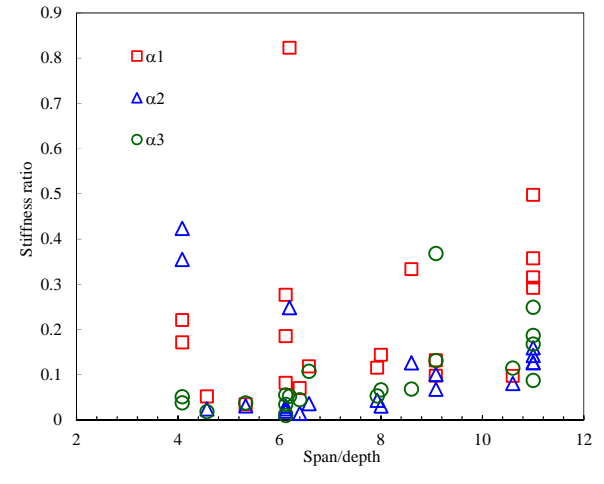
Two values of ductility demand, μ , can be resolved from Eq.(8). The one larger than μ_c , denoted as μ_r , is the ductility demand for the effective catenary action. Its corresponding rotation is designated as θ_r in Fig. 2(b).

Parametric study

From the previous derivation, it was observed that the chord rotation demand for the effective catenary action was involved with several parameters, which included the three stiffness ratios and chord rotations of the static arch resistance and leveled off point. The stiffness ratios were influenced by the span-to-depth ratio, reinforcement details, material strength, and boundary constraints of the members bridging the removed column. Fig. 3 shows the variations of α_1 , α_2 , and α_3 with the span-to-depth ratio, which were estimated from several published test results [Su et al. (2009); Yu and Tan (2013); Lew et al. (2014); Tsai et al. (2013, 2014)]. They were calculated by using the static peak arch, leveled off, and maximum catenary response prior to bar fracture. It is observed that most of the stiffness ratios varied from 0.1 to 0.3 for α_1 , from 0.05 to 0.15 for α_2 , and from 0.05 to 0.2 for α_3 . Therefore, the stiffness ratios considered in this study were determined as shown in Table 1. In the referred experimental results, a larger span-to-depth ratio generally led to a larger α_1 . However, the corresponding chord rotation of peak arch resistance decreased with increased span-to-depth ratio.

Table 1 Stiffness ratios of the three phases for the parametric study

α_1	α_2	α_3
0.1	0.05 ~ 0.15 @ 0.05	0.05 ~ 0.2 @ 0.05
0.2	$0.05 \sim 0.15 @ 0.05$	$0.05 \sim 0.2 @ 0.05$



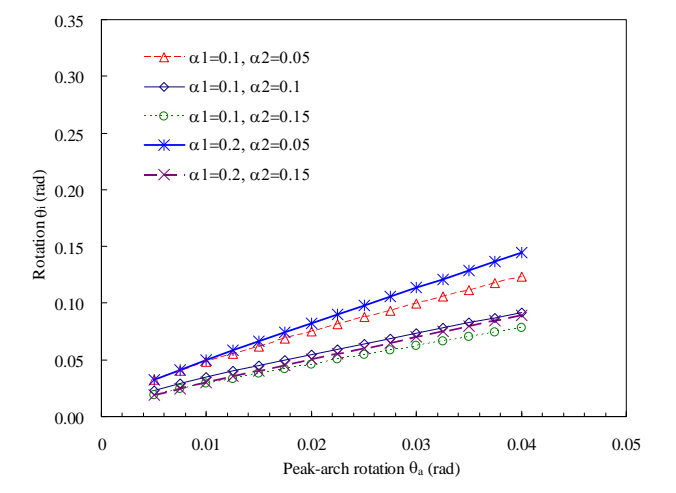


Figure 3 Variation of stiffness ratios estimated from published test results

Figure 4 Variation of snap-through prevention rotations

In order to investigate the chord rotation demand for the effective catenary action, it was assumed that the static leveled-off strength $P_c=0.5P_y$. This assumption was made to confirm that the pseudo-static peak arch resistance ($P_{p,a}$) occurred by the end of the transition phase. Then the leveled-off ductility was obtained as

$$\mu_c = \frac{0.5 + \alpha_1(\mu_a - 1) + \alpha_2 \mu_a}{\alpha_2} \tag{9}$$

The corresponding leveled-off rotation is determined from the product of the yield rotation θ_y and μ_c . The yield rotation was assumed as 0.005 rads [FEMA (2000)] in this study. According to the selected stiffness ratios in Table 1, the variations of the snap-through prevention rotation (θ_i) under

five different combinations of α_1 and α_2 are shown in Fig. 4. As implied in Eq.(7), it is observed that an increased θ_a could induce a larger snap-through prevention limit. Effect of the softening stiffness ratio is opposite to that of the arch stiffness ratio on θ_i , which appears more sensitive to the former. Fig. 5(a) shows the comparison of the minimum rotation demands (θ_r) for effective catenary action under five different parametric combinations with $\alpha_1 = 0.1$. The corresponding snap-through response, which was obtained from ($\theta_r - \theta_i$), is shown in Fig. 5(b). These figures reveal that the rotation demands of both the effective catenary action and snap-through response decreased with increased softening and catenary stiffness ratios. However, they increased with the peak arch rotation. This means that if the snap-through behavior is delayed, more plastic deformation must be developed for the effective catenary action.

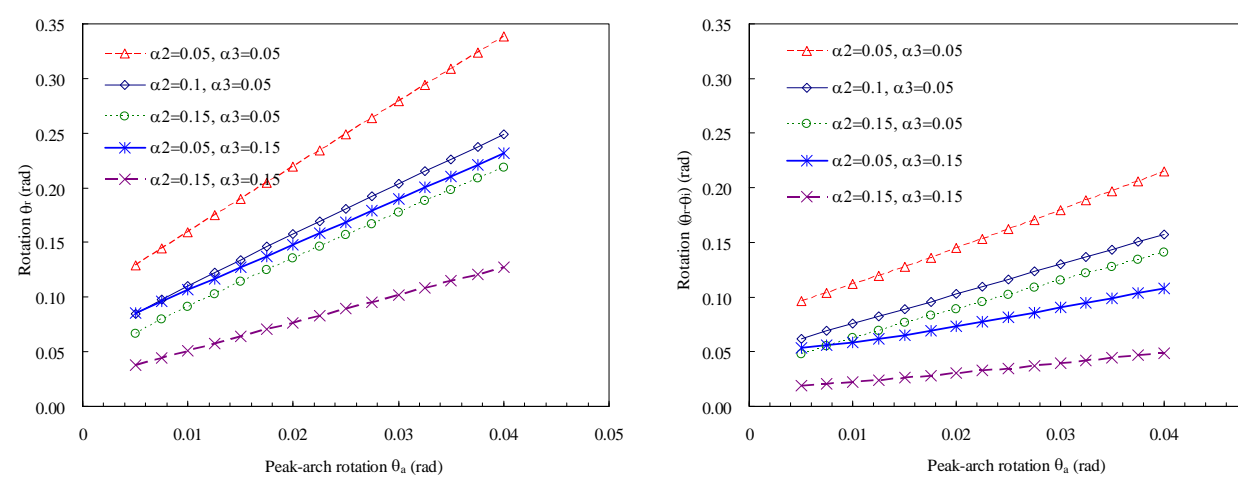


Figure 5(a) Minimum rotation demands (θ_r) for effective catenary action with $\alpha_1 = 0.1$

Figure 5(b) Snap-through rotation (θ_r - θ_i) with $\alpha_1 = 0.1$

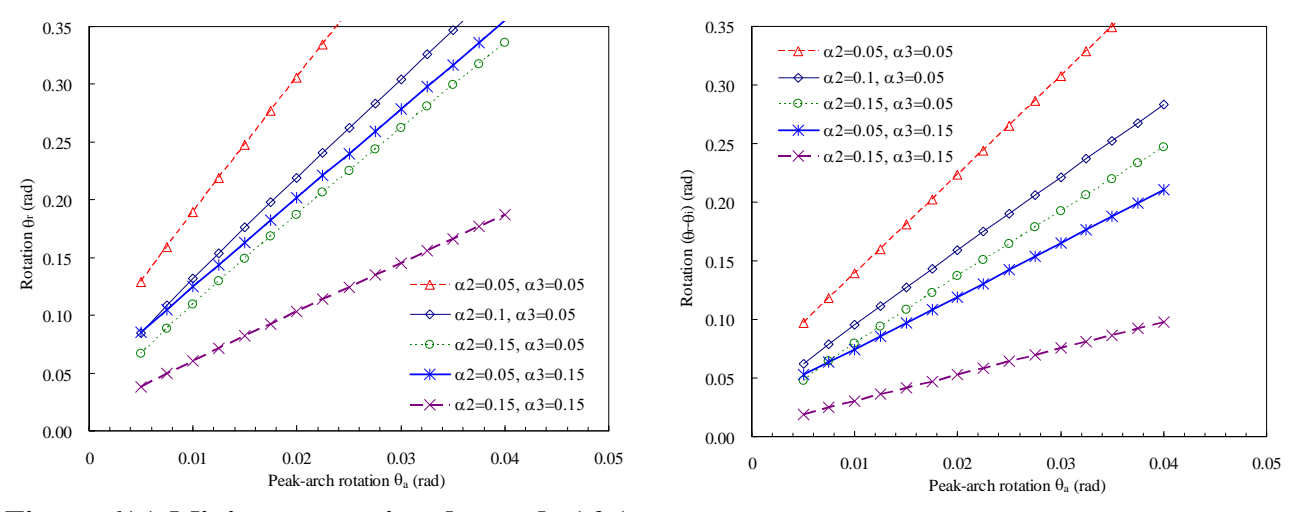


Figure 6(a) Minimum rotation demands (θ_r) for effective catenary action with $\alpha_1 = 0.2$

Figure 6(b) Snap-through rotation ($\theta_r - \theta_i$) with $\alpha_1 = 0.2$

It is noted that a large α_2 represents swifter stiffness degradation in the transition phase and thus an earlier activation of the catenary action. It may occur in members suffered from shear failure during the gravitational monotonic loading process [Tsai et al. (2013)]. Also, it is observed that both α_2

and α_3 had similar influence in the rotation demands of effective catenary action and snap-through response. Either increasing α_2 from 0.05 to 0.15 with α_3 = 0.05 or α_3 from 0.05 to 0.15 with α_2 = 0.05 could result in approximate rotational reduction. As indicated in some test results, larger peakarch rotation and smaller α_2 were generally resulted from specimens with a deeper section. This implies that more critical chord rotation demand may be advised under such conditions. The acceptance criterion of 0.20 radians, which is regarded as the minimum demand for catenary development as recommended in the UFC guidelines, may not be always conservative for the RC beams with a deep section.

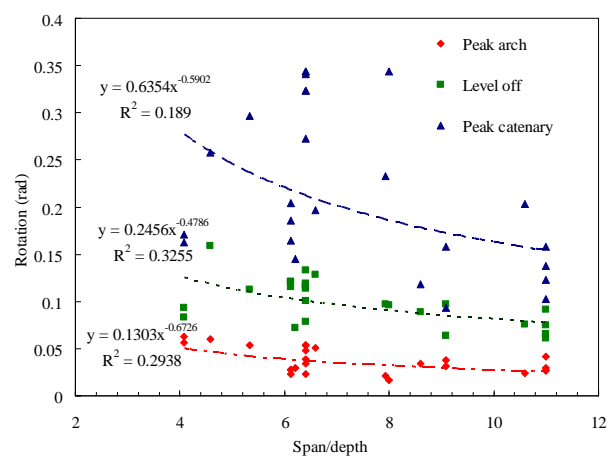


Figure 7 Experimental variations of the threshold chord rotations (estimated from the referred test results)

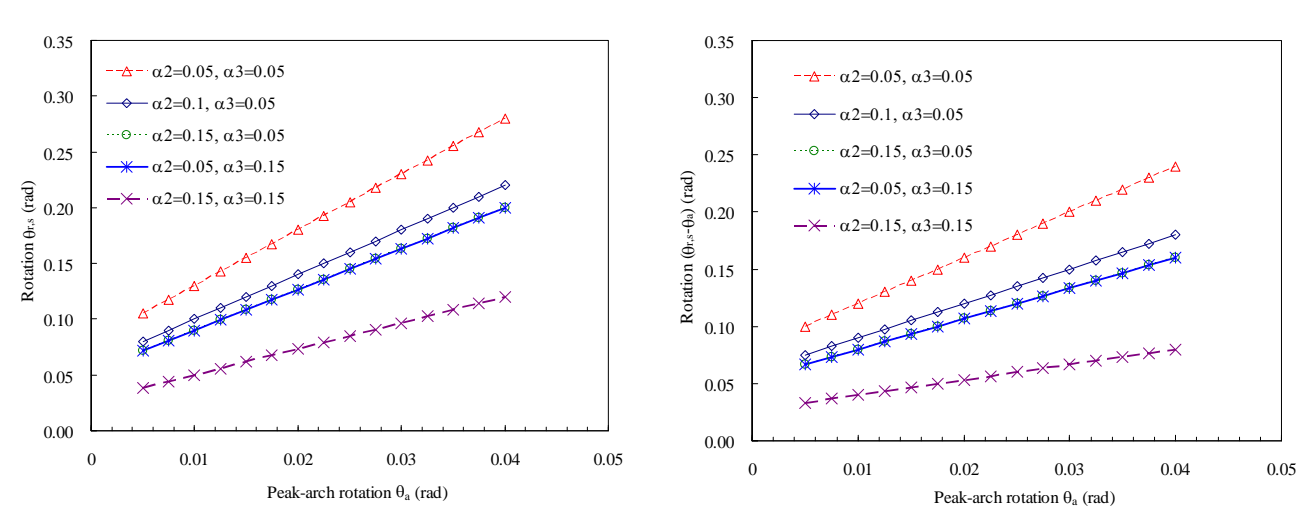


Figure 8(a) Static rotation demands for the effective catenary action

Figure 8(b) Static rotation demands for the snap-through response

Figs. 6(a) and 6(b) show the chord rotations for effective catenary action and snap-through response with a larger arch stiffness ratio, $\alpha_1=0.2$. Compared with the corresponding Figs. 5(a) and 5(b), it is observed that a larger arch stiffness ratio may increase the rotation demands for effective catenary action, snap-through prevention limit, and snap-through deformation. From the referred test results, a larger span-to-depth ratio generally led to increased arch and catenary stiffness ratios, as observed from Fig. 3. Thus, the adverse influence of the increased arch stiffness on the chord rotation demand may be partially mitigated by the increased catenary stiffness. Also, from the

experimentally observed variations of the threshold chord rotations, as shown in Fig. 7, the rotation at peak arch resistance decreased with increased span-to-depth ratios. This could further reduce the rotation demands of effective catenary action and snap-through response for RC beams with a larger span-to-depth ratio. These observations explain why RC beams with shallower sections usually present earlier triggered catenary actions.

Although dynamic tests may reflect the realistic column-loss scenarios, the experimental costs for test setup and instrumentation are usually larger than conventional static tests. Hence, there were more experimental studies conducted with static tests. From the idealized piece-wise linear curve, a ductility demand for statically effective catenary action may be obtained from $P_a = P_u$. The resulting static rotation demand is written as

$$\theta_{r,s} = \theta_y \frac{(\alpha_2 + \alpha_3)\mu_c - \alpha_2\mu_a}{\alpha_3} \tag{10}$$

Different from the pseudo-static rotation demand obtained from Eq.(8), the static rotation is independent of the arch stiffness ratio. Figs. 8(a) and 8(b) show the static rotation demands for the effective catenary action and snap-through response based on Eq.(10). The comparison of Figs. 8 and Figs. 5 indicates that the rotation demand, either for the effective catenary action or the snap-through response, may be underestimated if based on the nonlinear static response only. Hence, if the static monotonic test results of RC beams present a recovery of the static peak arch resistance in the catenary phase, complementary pseudo-static analysis is necessary to verify the effective catenary action under realistic dynamic column loss.

Conclusions

Because of the widespread attention paid to the progressive collapse resistance of building structures under column loss, chord rotation demands for the effective catenary action of RC beams were investigated in this study. The nonlinear static response of RC beams under monotonic pushdown loadings was idealized as a piece-wise linear curve with four threshold points. Based on the idealized static response, analytical formulations were derived to determine the pseudo-static chord rotation for the effective catenary action and accompanied snap-through response. The numerical parametric studies revealed that the minimum rotation demand of 0.20 radians recommended in the UFC guidelines for catenary development was not always conservative. Larger peak-arch rotation and smaller catenary stiffness may increase the rotation demand for effective catenary action. This implied that RC beams with a deep section may need higher rotation capacity for catenary development. Since RC members with a deep section are usually responsible of large shear and/or moment, it is suggested to adopt their peak arch strength as the collapse resistance for the sake of safety. Also, a peak-arch strength recovery in the nonlinear static response curve does not always guarantee a similar strength recovery in the pseudo-static counterpart. Complementary pseudo-static analysis is advised to verify the effective catenary action under realistic dynamic column loss. In general, a combination of smaller arch stiffness, larger softening stiffness, and larger catenary stiffness may lead to an earlier strength recovery in the catenary phase. Since the arch, softening, and catenary stiffness are involved with the span-to-depth ratio, main reinforcement ratio and layout, shear reinforcement, and boundary constraint of the RC members, it will be an important task to clarify their relationships in future studies.

References

ASCE (2010) Minimum Design Loads for Buildings and Other Structures, ASCE/SEI 7-10, American Society of Civil Engineers, Reston, Virginia.

Choi, H. and Kim, J. (2011) Progressive collapse-resisting capacity of RC beam-column sub-assemblage, *Magazine of Concrete Research* **63**, 297-310.

- DoD (Department of Defense) (2005) Design of Buildings to Resist Progressive Collapse, UFC 4-023-03, Washington, DC, USA.
- DoD (Department of Defense) (2009) Design of Buildings to Resist Progressive Collapse, UFC 4-023-03, Washington, DC, USA.
- FEMA (2000) Prestandard and Commentary for the Seismic Rehabilitation of Buildings, FEMA-356, Federal Emergency Management Agency, Washington, DC, USA.
- GSA (General Service Administration) (2003) Progressive Collapse Analysis and Design Guidelines for New Federal Office Buildings and Major Modernization Projects, Washington, DC, USA.
- Lew, H. S., Bao, Y., Pujol, S., and Sozen, M. A. (2014) Experimental study of reinforced concrete assemblages under column removal scenarios, *ACI Structural Journal* **111**(4), 881-892.
- Orton, S. and Kirby, J. (2014) Dynamic response of an RC frame under column removal, *Journal of Performance of Constructed Facilities* **28**(4), 04014010-1-8.
- Qian, K. and Li, B. (2012) Dynamic performance of reinforced concrete beam-column substructures under the scenario of the loss of a corner column experimental results, *Engineering Structures* **42**, 154-167.
- Sasani, M., Werner, A., and Kazemi, A. (2011) Bar fracture modelling in progressive collapse analysis of reinforced concrete structures, *Engineering Structures* **33**, 401-409.
- Su, Y., Tian, Y., and Song, X. (2009) Progressive collapse resistance of axially-restrained frame beams, *ACI Structural Journal* **106**(5), 600-607.
- Tian, Y. and Su, Y. (2011) Dynamic response of reinforced concrete beams following instantaneous removal of a bearing column, *International Journal of Concrete Structures and Materials* **5**(1), 19-28.
- Tsai, M. H. and Lin, B. H. (2008) Investigation of progressive collapse resistance and inelastic response for an earthquake-resistant RC building subjected to column failure, *Engineering Structures* **30**(12), 3619-3628.
- Tsai, M. H. (2010) An analytical methodology for the dynamic amplification factor in progressive collapse evaluation of building structures, *Mechanics Research Communications* **37**, 61-66.
- Tsai, M. H. and You, Z. K. (2012) Experimental evaluation of inelastic dynamic amplification factors for progressive collapse analysis under sudden support loss, *Mechanics Research Communications* **40**, 56-62.
- Tsai, M. H., Lu, J. K., and Chang, Y. T. (2013) Experimental investigation on the collapse resistance of RC beam-column sub-assemblages, *Proceeding the 6th Civil Engineering Conference in Asia Region*, Jakarta, Indonesia, August 20-22, TS8-35-41.
- Tsai, M. H., Lu, J. K., and Huang, B. H. (2014) Column-loss response of RC beam-column sub-assemblages with different bar-cutoff patterns, *Structural Engineering and Mechanics*, **49**(6), 775-792.
- Yu, J. and Tan, K. H. (2013) Structural behaviour of RC beam-column sub-assemblages under a middle column removal scenario. *Journal of Structural Engineering* 139(2), 233-250.